Astrocyte store-operated calcium entry is required for centrally mediated neuropathic pain

Mariya A. Prokhorenko and Jeremy T. Smyth

Supplementary Material

Supplemental Figure S1

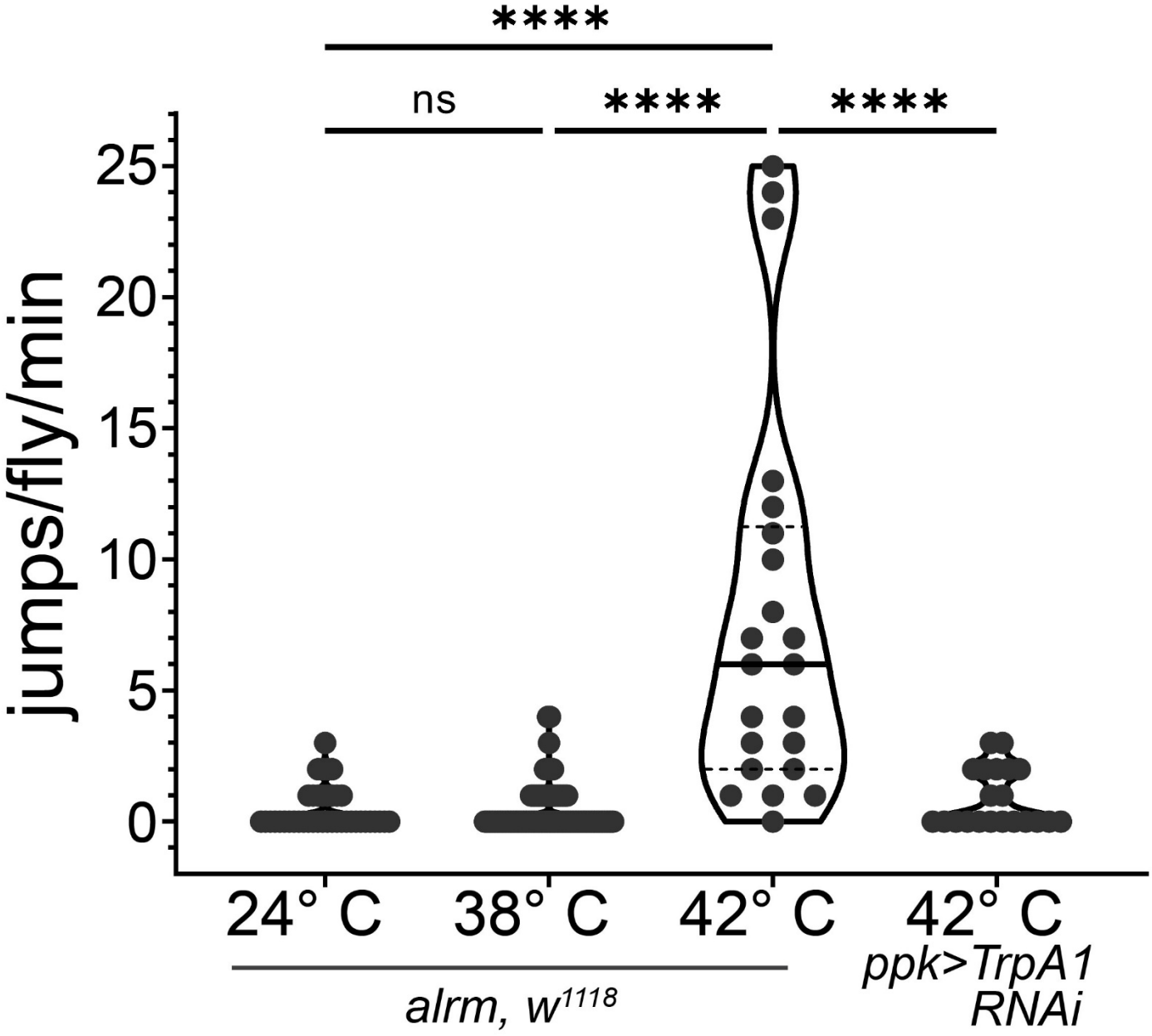

Supplemental Figure S1. Jumping response is antinociceptive and initiates at a threshold greater than 38° C in healthy flies. Plot of the number of jumps per fly per minute at 38° C for indicated genotypes and at indicated temperatures. All animals were uninjured. Each symbol represents the total number of jumps for a single animal (*n=42* for 24°, *n=93* for 38°, *n=22* for 42° *alrm-GAL4; w^{1118}* controls and *n=21* for *ppk>TrpA1 RNAi*). ****, P<0.0001; ns, not significant; Kruskal-Wallis with Dunn's multiple comparisons.

Supplemental Figure S2

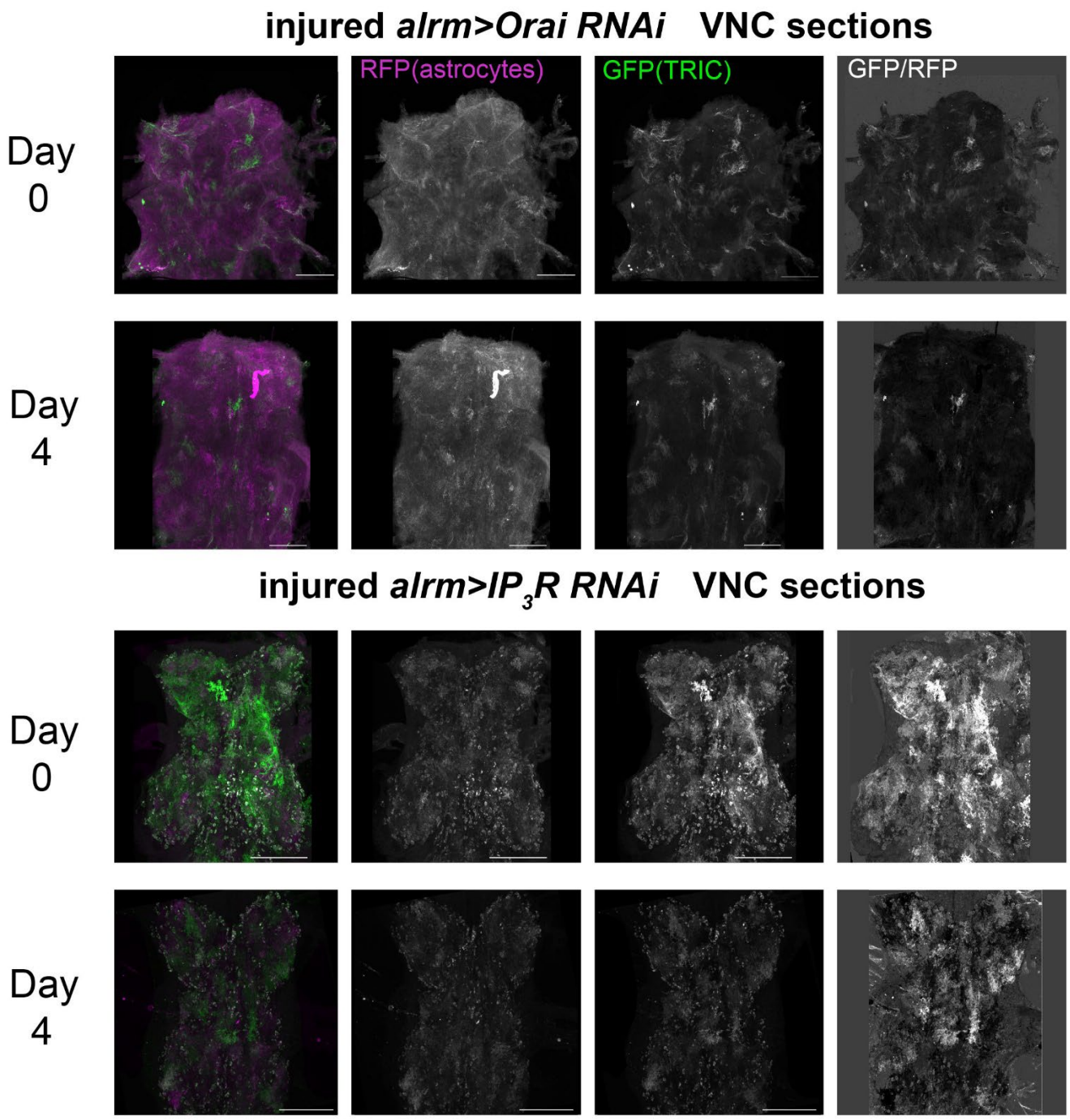

Supplemental Figure S2. Astrocyte Ca^{2+} signaling does not increase four days after injury if IP_3R or Orai is suppressed. Representative images of TRIC-mediated GFP fluorescence (green) and astrocyte-restricted RFP fluorescence (magenta) in VNCs from day 0 (uninjured) and day 4 post-injury *alrm-GAL4>Orai RNAi* and *alrm-GAL4>IP₃R RNAi* animals. Also shown are images of the product of GFP divided by RFP fluorescence, representative of the normalized Ca^{2+} signaling activity reported by TRIC.

Supplemental Figure S3

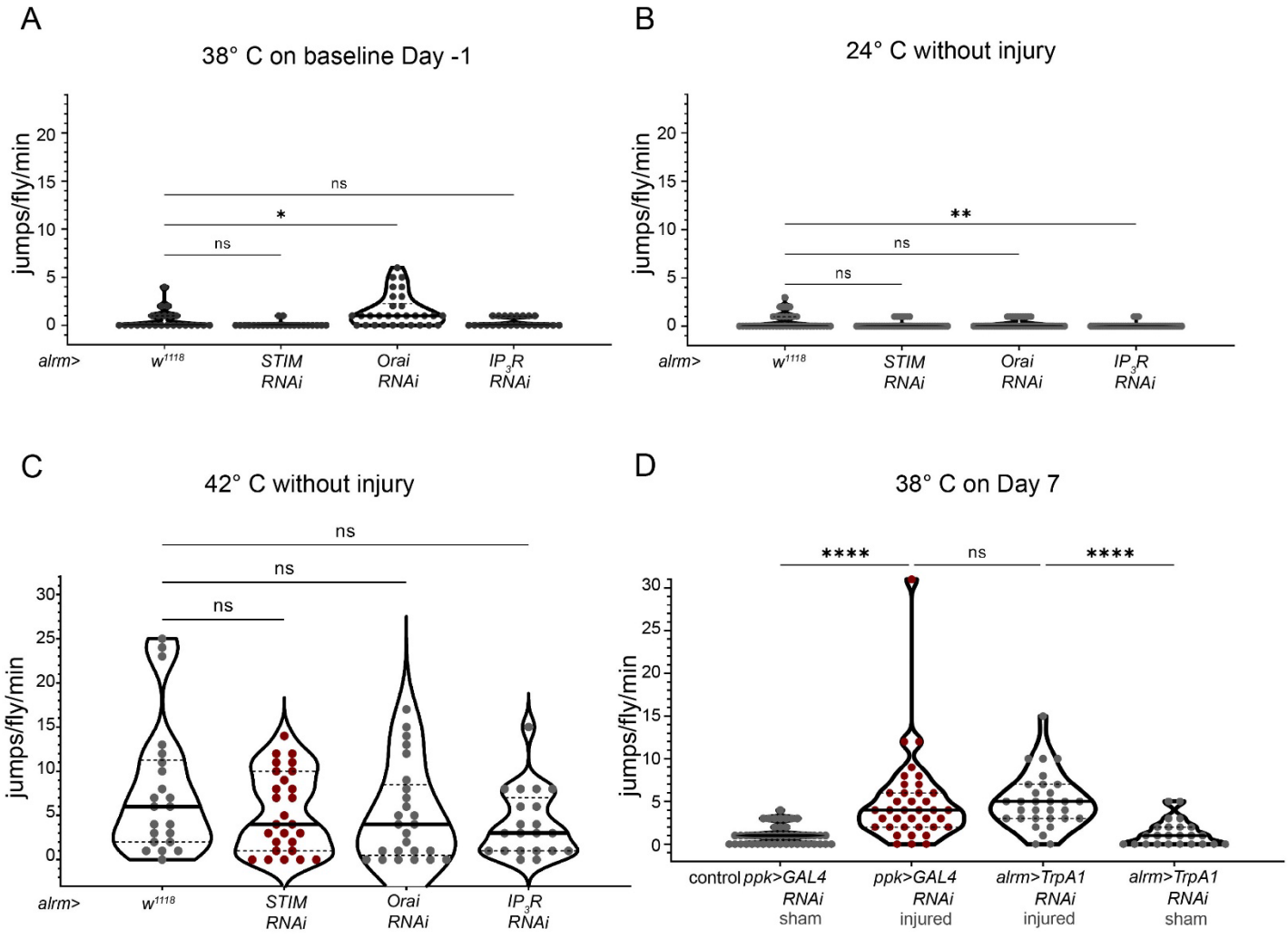

Supplemental Figure S3. Suppression of astrocyte store-operated calcium entry components does not alter normal jumping activity or nocifensive response to high temperature. (A) Plot of the number of jumps per fly per minute at 24° C for uninjured flies with indicated genotypes. **(B)** Plot of the number of jumps per fly per minute at 38° C for uninjured flies with indicated genotypes. **(C)** Plot of the number of jumps per fly per minute at 42° C for uninjured flies with indicated genotypes. **(D)** Plot of the number of jumps per fly per minute at 38° C for sham or seven-day injured flies with indicated genotypes. **0.01<P<0.05; **0.001<P<0.01; ****P<0.0001*; ns, not significant; Kruskal-Wallis with Dunn's multiple comparisons, *N=101, H(3)=22.08, P<0.0001, N=174, H(3)=9.871, P=0.0197, N=94, H(3)=3.267, P=0.3523, N=40, H(3)=58.85, P<0.0001* respectively.

Supplemental Figure S4

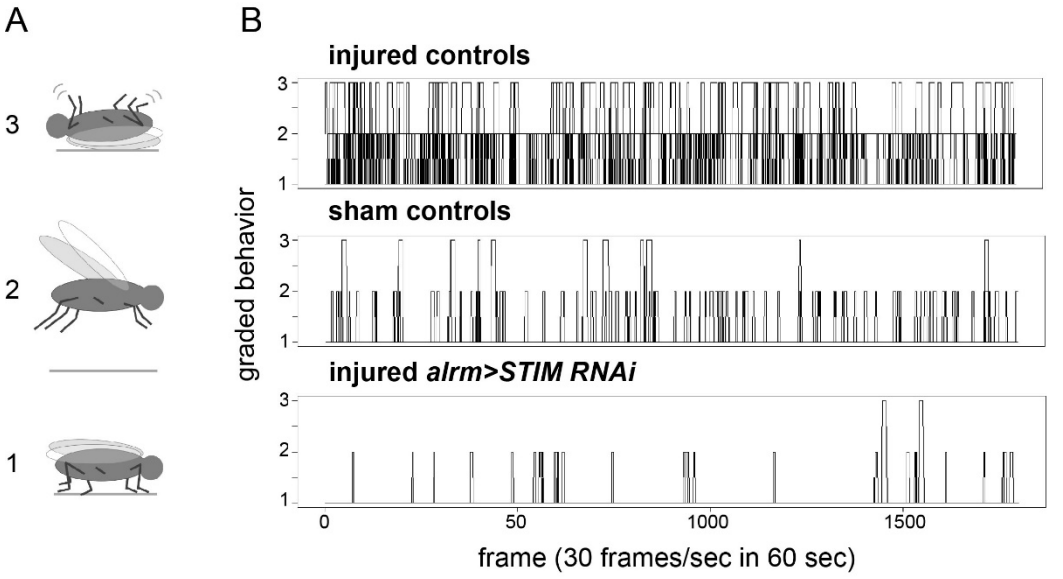

C

Test groups	LDA predictions: injured	LDA predictions: sham
alrm>GAL4 RNAi injured	15	6
ppk>GAL4 RNAi injured	50	8
alrm>IP3R RNAi injured	14	31
alrm>Orai RNAi injured	7	17
alrm>STIM RNAi injured	7	31

Supplemental Figure S4. Grading of fly behavior 7 days after injury for cepstral linear discriminant analysis. (A) For every frame of video (1800 frames in 1 minute at 30 frames per second), each fly's behavior was binned according to an ordinal scale depending on intensity of reaction to the thermal stimulus. 1=all behaviors not considered anti-nociceptive, 2= jumping, 3=rolling, not able to recover on feet. **(B)** 1-minute time series generated after binning behavior presented cumulatively per injured controls, sham controls, and STIM RNAi group. Individual fly time series are used as model input with identified conditions (injured or sham) for the training and deidentified for the testing **(C)** Linear discriminant model predictions from the test groups. All test groups are injured animals; *15/21 alrm>GAL4 RNAi* and *50/58 ppk>GAL4 RNAi* controls were categorized correctly as injured, *31/45 alrm>IP3R RNAi, 17/24 alrm>Orai RNAi*, and *31/38 alrm>STIM RNAi* were predicted to be sham despite injury.

Supplemental Figure S5

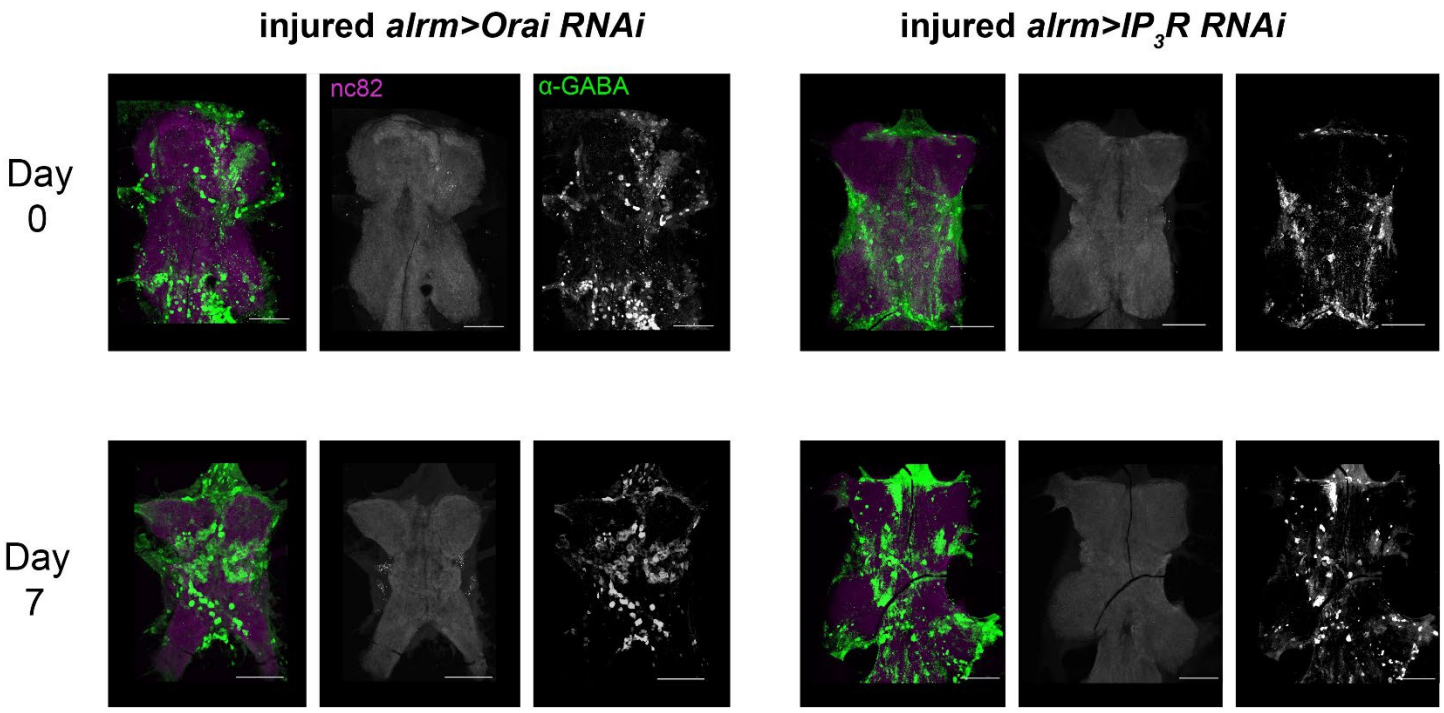

Supplemental Figure S5. GABAergic neuron loss following injury is prevented by astrocyte Orai and IP_3R suppression. Representative images of VNCs from day seven injured *alrm>Orai RNAi* (left) and *alrm>IP₃R RNAi* (right) animals labeled with antibodies to α-GABA (green) and Bruchpilot (magenta) to label synaptic active zones within the neuropil.

Supplemental Figure S6

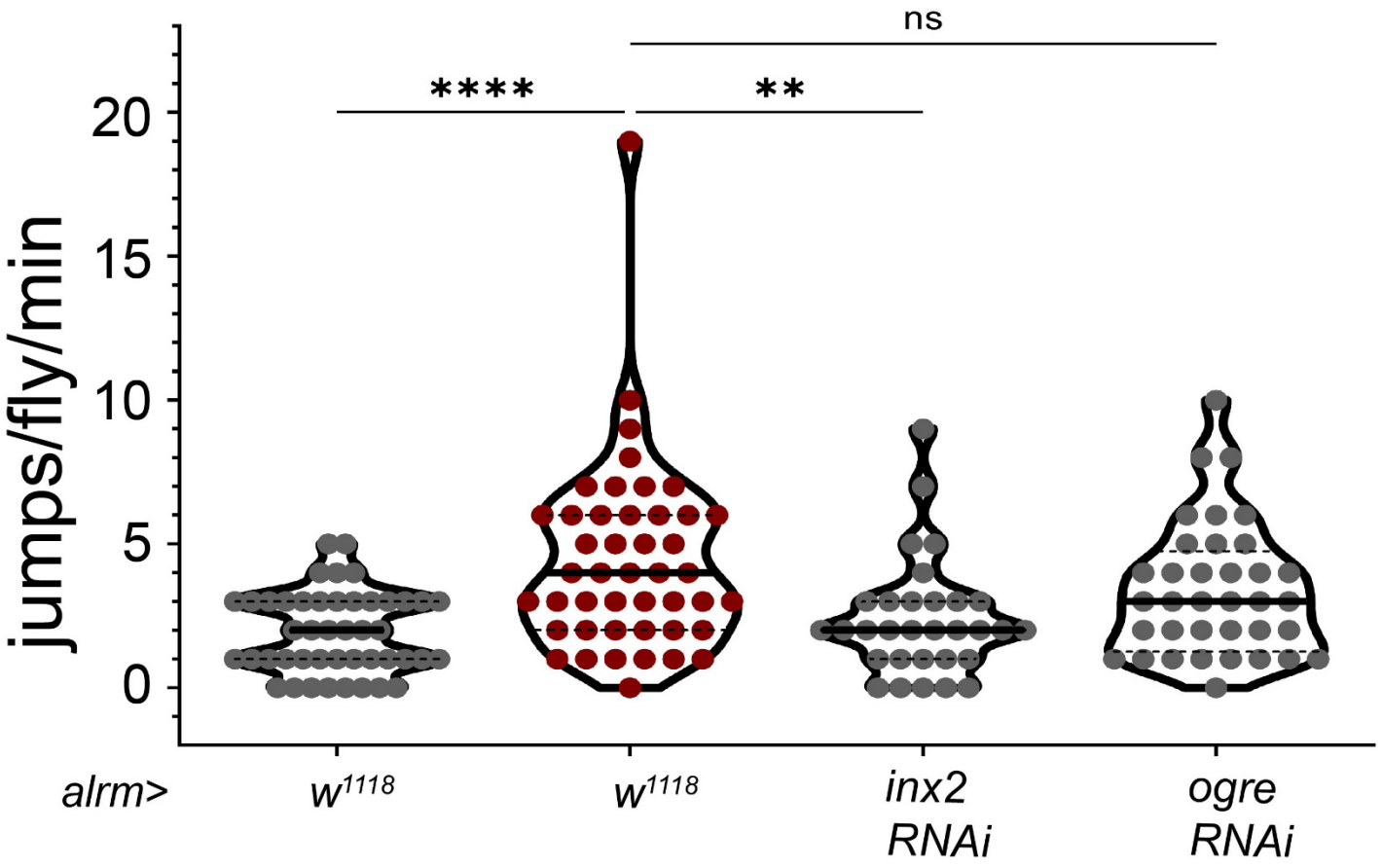

Supplemental Figure S6. Astrocyte gap junction subunit suppression prevents thermal hypersensitivity following injury. Plot of the number of jumps per fly per minute at 38° C for seven days following leg amputation injury ("injured") for the indicated genotypes. Each symbol represents the total number of jumps for a single animal (*n=45* for *alrm-GAL4; w^{1118}*, *n=31* for *alrm>inx2 RNAi, n=36* for *alrm>ogre RNAi,* and *n=45* for *alrm-GAL4; w^{1118}* sham controls) ****, *P<0.0001*; Kruskal-Wallis with Dunn's multiple comparisons, *N=157, H(3)=24.63, P<0.0001*.

Supplemental Figure S7

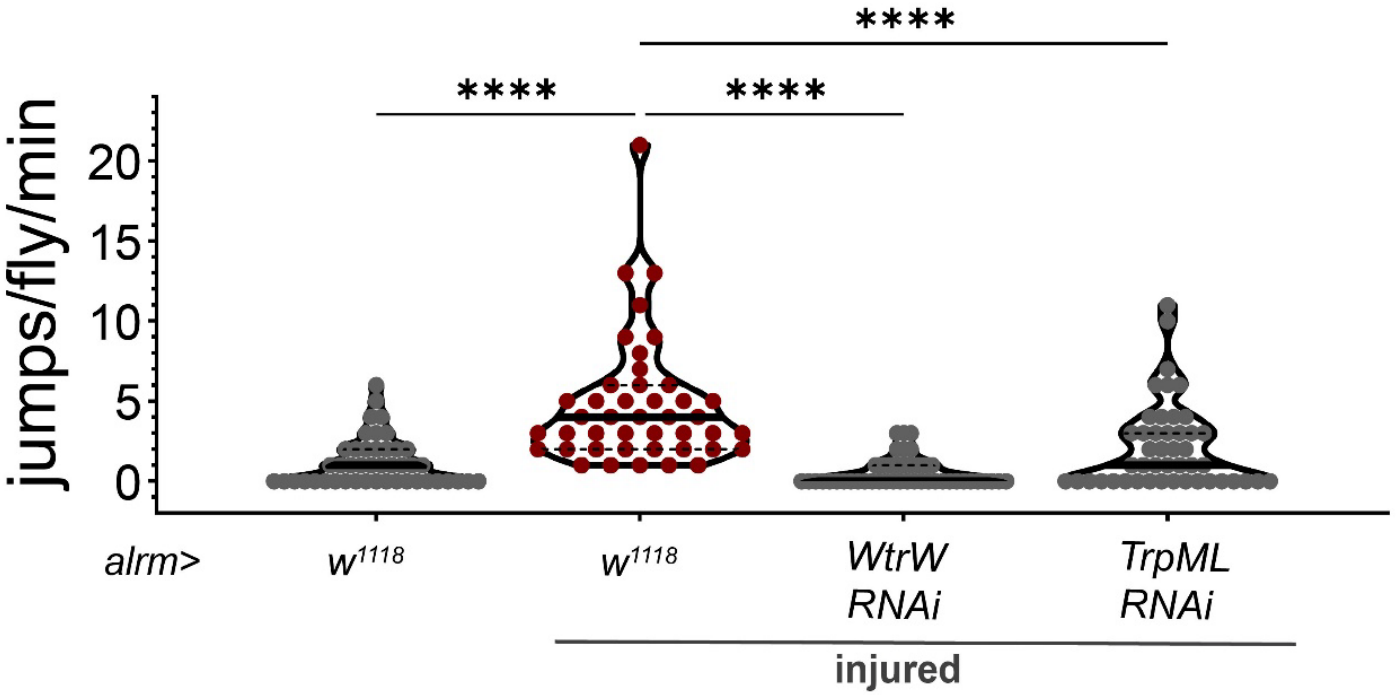

Supplemental Figure S7. Suppression of astrocyte Waterwitch and TrpML channels attenuates thermal hypersensitivity following injury. Plot of the number of jumps per fly per minute at 38° C for seven days following leg amputation injury ("injured") for the indicated genotypes. Each symbol represents the total number of jumps for a single animal (*n=43* for *alrm-GAL4; w^{1118}*, *n=45* for *alrm>Wtrw RNAi, n=46* for *alrm>TrpML RNAi* injured groups and *n=45* for *alrm-GAL4; w^{1118}* sham controls) ****, P<0.0001; Kruskal-Wallis with Dunn's multiple comparisons, *N=179, H(3)=64.62, P<0.0001*.

Supplemental Table 1. STAR Methods

Reagent or Resource	Source	Identifier
***Drosophila* Stocks**		
w[*]; P{w[+m*]=alrm-GAL4.D}3/CyO; Dr[1]/TM3, Sb[1]	BDSC RRID:SCR_006457 https://bdsc.indiana.edu/	astrocyte-like glia GAL4 driver stock# 67031
w[*]; wg[Sp-1]/CyO; P{w[+m*]=alrm-GAL4.D}2	BDSC RRID:SCR_006457 https://bdsc.indiana.edu/	astrocyte-like glia GAL4 driver stock# 67032
w[*]; P{w[+mC]=ppk-GAL4.G}2	BDSC RRID:SCR_006457 https://bdsc.indiana.edu/	pickpocket sensory neuron GAL4 driver stock# 32078
y[1] v[1]; P{y[+t7.7] v[+t1.8]=TRiP.JF02461}attP2	BDSC RRID:SCR_006457 https://bdsc.indiana.edu/	UAS TrpA1 RNAi stock# 36780
y[1] sc[*] v[1] sev[21]; P{y[+t7.7] v[+t1.8]=TRiP.HMC03562}attP40	BDSC RRID:SCR_006457 https://bdsc.indiana.edu/	UAS Orai RNAi stock# 53333
UAS-dOrai(G170M)/cyo, GFP	internal	UAS dOrai G170M
UASt-dOrai+/TM6, Tb	internal	UASt dOrai+
y[1] v[1]; P{y[+t7.7] v[+t1.8]=TRiP.JF01957}attP2	BDSC RRID:SCR_006457 https://bdsc.indiana.edu/	UAS Itpr RNAi stock# 25937
y[1] v[1]; P{y[+t7.7] v[+t1.8]=TRiP.JF02567}attP2	BDSC RRID:SCR_006457 https://bdsc.indiana.edu/	UAS Stim RNAi stock# 27263
w[*] P{y[+] w[+]=10XUAS-IVS-mCD8::RFP}attP18 P{y[+] w[+]=13XLexAop2-mCD8::GFP}su(Hw)attP8; P{y[+] w[+]=UAS-MKII::nlsLexADBDo}attP40, P{y[+] w[+]=UAS-p65AD::CaM}attP24/CyO; M{w[+]=UAS-p65AD::CaM}ZH-86Fb	BDSC RRID:SCR_006457 https://bdsc.indiana.edu/	TRIC LexAop mCD8-tagged GFP, UAS mCD8-tagged RFP; UAS lexA(DBD)::CaMTP, UAS p65(AD)::CaM; UAS p65(AD)::CaM stock# 62827
y[1] sc[*] v[1] sev[21]; P{y[+t7.7] v[+t1.8]=VALIUM20-GAL4.2}attP2	BDSC RRID:SCR_006457 https://bdsc.indiana.edu/	UAS GAL4 RNAi stock# 35783
Immunohistochemistry		
Mouse Bruchpilot nc82-s	DSHB	Cat# nc82, 4/16/20 RRID:AB_2314866
Rabbit Living colors dsRed	Takara Bio	Cat#632496, Lot 2103116

		RRID:AB_10013483
Rabbit anti-GABA	Sigma	Cat#0000154656
Chicken anti-GFP	Abcam	Cat#AB13970
Alexa fluor 488 goat anti-chicken	Invitrogen	Cat#A11039, Lot 1637891
Alexa fluor 568 goat anti-rabbit	Invitrogen	Cat#A11011, Lot 2379475
Alexa fluor 488 goat anti-rabbit	Invitrogen	Cat#A11008, Lot 2420731
Alexa fluor 568 goat anti-mouse	Invitrogen	Cat#A11004, Lot 2332536
Mounting Reagents		
Kodak Photo-Flo 200 Solution	Electron Microscopy Sciences	Cat#74257
Poly-L-lysine hydrobromide (PLL)	Sigma	Cat#P1524-25MG
DPX mountant for microscopy	Electron Microscopy Sciences	Cat# 13512
Ethanol >99.5% (200 proof)	Sigma	Cat# 459844-1L
Paraformaldehyde (PFA) 16% Aqueous Solution	Electron Microscopy Sciences	Cat#15710
Phosphate buffered saline (PBS) 1X	Cellgro	Cat#21-040
Triton X-100	Sigma	Cat#X100
Sylgard 184 silicone elastomer kit	Sigma	Cat# 761028-5EA
Schneider's Insect Medium (S2)	Fisher Scientific	Cat#21720-024
Fetal Bovine Serum		Cat#
Software		
MATLAB (R2019B)	www.mathworks.com/matlab	RRID:SCR_001622
Fiji	http://fiji.sc	RRID:SCR_002285
R (4.2.2)	https://cran.r-project.org/	RRID:SCR_001905
CepLDA (R package)	(Krafty, RT, 2016)	
GraphPad Prism (9.5.0 (730)	www.graphpad.com	RRID:SCR_002798
Deposited data		
Raw and analyzed data	Figshare	
Analyzed data and codes	GitHub	
Equipment		
Nikon A1R Confocal Laser Microscope	www.microscope.healthcare.nikon.com	RRID:SCR_020318
Thermal testing 3 mm ring	GitHub	
Vellum translucent paper	Staples	Cat#496755
Isoblock Dry Bath Incubator	Benchmark Scientific	SKU#BSH6000
Fisherbrand Traceable Infrared Thermometer Gun	Fisher Scientific	

Wide 28 mm 77° f/1.7 lens video camera with Sony Exmor IMX363 12.2-megapixel sensor	https://store.google.com	Pixel 4
Dumont #5 forceps	Fine Science Tools	Cat#11252-20
Corning cover glass No.1	Fisher Scientific	Cat#12-553-451